IN-ORBIT DEMONSTRATION OF THE WORLD'S SMALLEST LASER COMMNUNICATION TERMINAL – OSIRIS4CUBESAT / CUBELCT

Benjamin Rödiger [(1)], Christopher Schmidt [(1)]

[(1)] German Aerospace Center (DLR), Institute of Communications and Navigation, Muenchener Strasse 20, 82234 Wessling, GERMANY, +498153282944,
benjamin.roediger@dlr.de

ABSTRACT

Free space optical communication is on its way to transform satellite communication. With its high data rates, robustness against electromagnetic interferences and license free secure channels, it overcomes the capabilities of classical radio channels. Especially small satellites require compact and efficient communication solutions. Thus, German aerospace center developed the world's smallest laser communication terminal OSIRIS4CubeSat, which is already advertised by Tesat Spacecom under the name CubeLCT [1].

This paper describes the first demonstrator mission PIXL-1 and the in-orbit verification of OSIRIS4CubeSat. It gives an overview of the space and ground system and depicts the operations concept. The paper discusses the challenges during the mission, especially the dependencies on the pointing accuracy and the reliability of the attitude determination and control System of the satellite. Furthermore, first results of the mission are discussed. The PIXL-1 mission finished successfully with a picture transmission in a quasi-operational scenario where a full end-to-end communication chain could be demonstrated. This includes taking and encoding the picture, transferring it via laser to the optical ground station Oberpfaffenhofen – next generation and decode it on ground.

1 INTRODUCTION

Efficient and compact sensors generate a huge amount of data, even on smallest satellites. With the increasing number of spacecrafts due to the trend towards (mega-)constellations, inventive solutions are required to overcome the bottleneck in communication. The physical limitations of radio-frequency (RF) channels induce research in other technological areas. Free space optical (FSO) communication provides such solutions to overcome these obstacles. One of the key factors of FSO are the very narrow opening angles (divergences) of laser beams, which increases the power density at the receiver and leads to extremely high data-rates and very efficient designs.

On the other hand, low divergences require very accurate pointing. Small satellites like CubeSats are limited in their accuracy which is usually lower than the divergence of the laser. Thus, a fine pointing assembly (FPA) is required to compensate the inaccuracies of the spacecraft. The pointing acquisition and tracking (PAT) concept is a commonly used procedure to actively control the beam steering in a very high accuracy.

FSO from small satellites was already demonstrated on experimental level in several missions [2][3]. OSIRIS4CubeSat (O4C) was developed together with Tesat Spacecom who provides the terminal under the name CubeLCT. The commercial interest in laser communication on CubeSats leads to the goal of the PIXL-1 mission to demonstrate the capabilities of O4C in a quasi- operational scenario. It was intended to demonstrate the capabilities in a scenario as close as possible to a theoretical, customer's use case.

2 SPACE SEGMENT

The goal of the OSIRIS4CubeSat project was to not only to design and integrate the payload, but also to verify it in a realistic environment. This led to a demonstrator mission in space. Therefore, PIXL-1 was planned as part of the project which includes a space platform containing a full qualified flight model of O4C.

2.1 OSIRIS4CubeSat

O4C is designed as a pure transmitter to send data from a satellite to the ground via laser. The goal was a miniaturized laser communication terminal design and pushing the systems capabilities to the physical limits. To achieve the maximum possible data-rate, the highest possible power density is required. This can be reached by designing a diffraction-limited optical system which transmits the laser at its physical lowest possible divergence. According to Eq. 1, with the given clear aperture of d = 14.47 mm, the divergence (full width half max, FWHM) of O4C is θ = 120 µrad (for λ = 1550 nm and M^2 = 1.2).

$$\theta = 2 \cdot \frac{\lambda}{\pi \cdot \frac{d}{\sqrt{2}}} \cdot M^2 \tag{1}$$

At the beginning of the project, typical CubeSat busses could reach a pointing stability with an absolute pointing error (APE) of up to 1° during target pointing mode. The divergence of O4C is with 120 µrad = 0.00688° much lower than the achievable pointing accuracy of a CubeSat. Thus, O4C is designed with a fine pointing assembly (FPA) to compensate the resulting difference in a closed control loop, which is depicted in Figure 1.

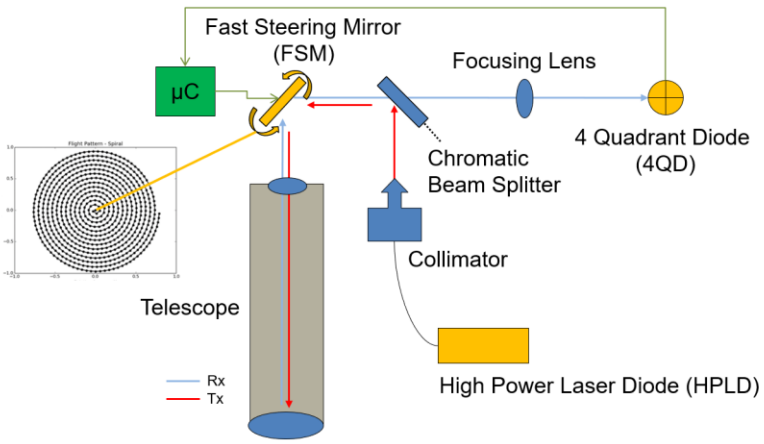

Figure 1. Block diagram of fine pointing assembly (FPA) inside O4C

The operation concept of O4C considers a combination of body pointing and closed loop tracking. To establish a connection, the terminal uses the Pointing Acquisition and Tracking (PAT) system which is illustrated in Figure 2. Therefore, a relatively broad beacon is sent from an Optical Ground Station (OGS), illuminates the satellite, a 4-Quadrant Diode (4QD) as a tracking sensor inside acquires the beacon, measures the angular error and a Fine Steering Mirror (FSM) corrects this error. To acquire the beacon, the FSM searches for it by driving spirals in the Field of Regard (FoR) of the terminal. Due to the ability of CubeSat busses having an APE of maximum 1° the radius of the FoR is equal to this APE, ±1° ex-aperture in each axis. This means the satellite has to point with an accuracy of better than 1° to the OGS during the whole transmission.

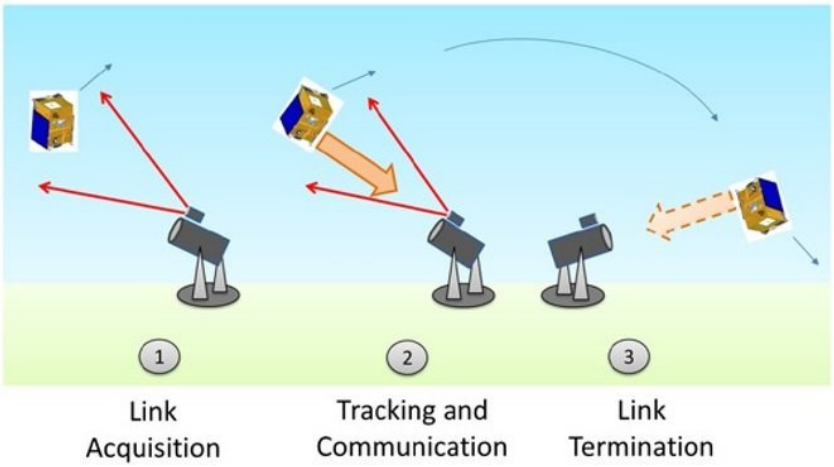

Figure 2. Illustration of the Pointing Acquisition and Tracking (PAT) concept [4]

The FPA is controlled by a microcontroller on the mainboard of the terminal. To achieve a highly compact and efficient design, intensive calculations like channel coding were outsourced to the satellites software defined radio (SDR). The user data, which have to be transmitted via laser are sent over a low voltage differential signal (LVDS) interface to the O4C terminal, which does the electrical-optical conversion.

2.2 CubeL

The goal of PIXL-1 was to verify the functionalities of O4C in a scenario which is as close as possible to a commercial use case. 3U is still today the most launched configuration of CubeSats thus, we decided to fly the first mission on board a 3U CubeSat [5]. Figure 3 depicts the single payloads and subsystems of which the most important are explained in the following chapter.

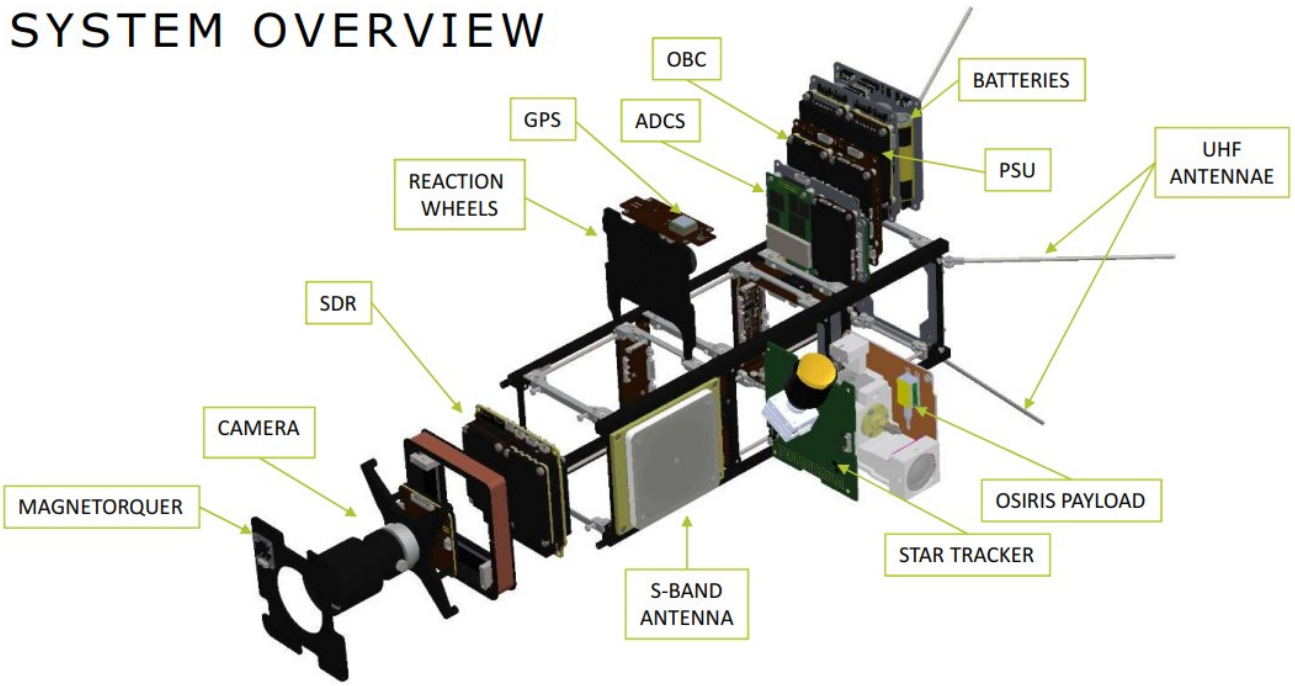

Figure 3. System Overview of CubeL

One of the most crucial subsystems is the attitude determination and control system (ADCS). The ADCS contains several sensors:

- Star tracker – absolute fine sensor
- Magnetometer – absolute coarse sensor
- Sun sensor – absolute coarse sensor
- GPS – position sensor
- Gyroscope – relative fine sensor

The inputs of the sensors are fed into a Kalman-filter which controls the satellite's attitude. If available, the main sensor for the Kalman-filter is the star tracker as it is the most accurate sensor with an accuracy of 10 arcsec (pitch & yaw) and 70 arcsec (roll), according to the data sheet. If the star tracker is not available the Kalman-filter continues with the last known quaternions, lowers down the weight of the sensor and increases the weight of the magnetometer input, as a secondary absolute sensor. The actuators are reaction wheels in a 4-wheel configuration to compensate zero-crossing. Furthermore, the satellite is equipped with a magnetorquer to desaturate the reaction wheels. CubeL has no propulsion system or thruster.

The mostly used purpose for satellites in low earth orbit (LEO) is Earth observation. To be as close to an operational scenario, CubeL is equipped with an RGB-camera, a NanoCam C1U from GomSpace. With a 70 mm lens the C1U has a ground sampling distance (GSD) of 30 m in a 650 km distance. High resolution pictures generate a huge amount of data. This is the most efficient way to demonstrate the capabilities and advantages of optical communication. The camera is directly connected to the SDR over a serial interface.

3 GROUND SEGMENT

During the PIXL-1 mission downlinks to several optical ground stations were tried. The paper concentrates on the optical ground station Oberpfaffenhofen – next generation (OGSOP-NG), as the major results were achieved with this ground station. The beacon and receiver system are identical to the ones used in the other OGS.

3.1 OGSOP-NG

The OGSOP-NG is especially designed for channel measurements of the atmospheric conditions. It is able to receive optical signals from geostationary and LEO satellites as well as aircrafts. The primary mirror has a diameter of 80 cm. The major improvement of the OGSOP-NG is the coudé-path. With three Nasmyth-ports, the received signal can be coupled out of the telescope and reflected through a vacuum tube into a laboratory below the OGS. This increases the flexibility of the OGS significantly and allows to permanently install many different measurement devices for distinguished purposes. Figure 4 shows the concept of the coudé-path [6].

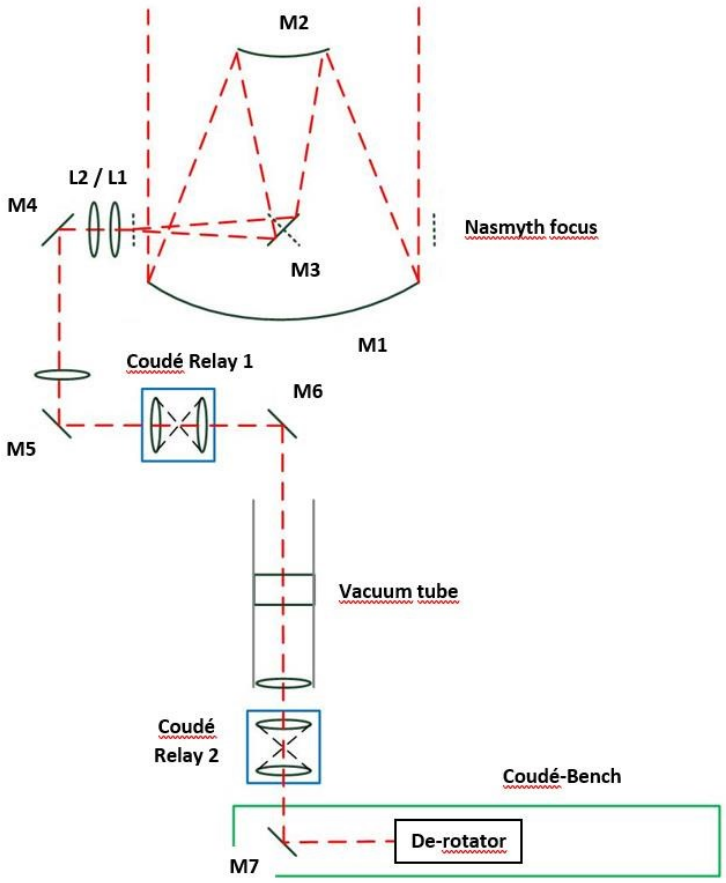

Figure 4. Coudé-path of OGSOP-NG [6]

Even though the OGSOP-NG is specially designed for atmospheric measurements it has the ability to receive operational data. This flexible concept makes it usable in the PIXL-1 mission.

3.2 Beacon System

As described in chapter 2.1, O4C makes use of the PAT concept to control the FPA. The OGSOP-NG is equipped with an Optical and Electrical Ground Support Equipment (OGSE and EGSE) to generate the beacons with the required optical power. Two beacons are used in a distance of 70 cm. This transmitter diversity is required to achieve decorrelated atmospheric channels and improve the optical uplink quality [7].

Transmission (Tx) and receiving (Rx) beam are separated by wavelength inside O4C. While the transmission laser is in the C-band (1550 nm) the beacons operate in the L-band (1590 nm). This relatively high distance between the wavelengths allows an easy optical separation of Tx- and Rx-beam in the terminal on the spacecraft. The beacon signal is modulated with a 10 kHz sine and demodulated in O4C to distinguish the beacon from stray light or reflections like the Earth albedo.

The OGSOP-NG points to and follows the satellite based on orbit files. Highly accurate orbit files based on GPS data from the satellite can achieve a very high accuracy of several ten meters. Nevertheless, the along-track error rises exponentially over time. The design goal was to select collimators with a divergence large enough, that the satellite is still in the illumination cone, even after considering the inaccuracies of the OGSOP-NG based on the propagated error of the orbit file. Simulated predictions show that the along-track error of commonly used orbit files is in the order of 160 m after 24 hours as it can be seen in Figure 5. Orbit files are generated once or twice per day.

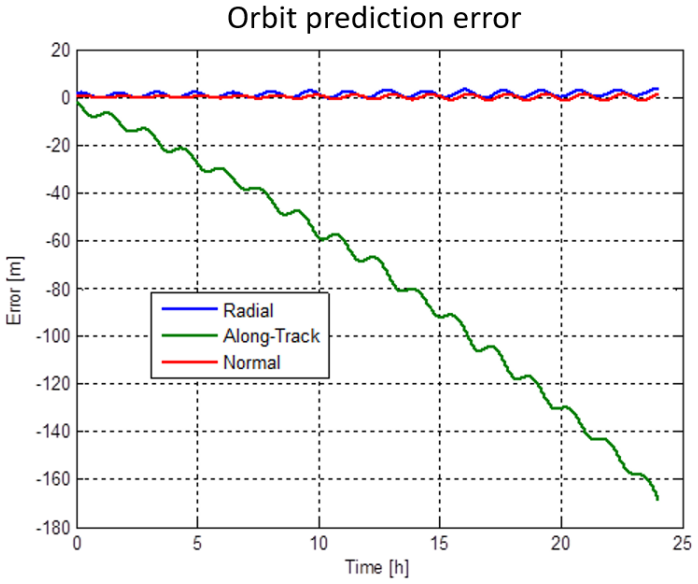

Figure 5. Error propagation of orbit files over time

Transmitter collimators with a divergence of θ = 1 mrad were selected. This leads according to Eq. 2 to a spot radius of r = 250 m, if the satellite is in l = 500 km distance (90° elevation flyover). The assumed maximum prediction error, according to Figure 5, is 160 m after 24 hours. With a spot radius of 250 m we still have 90 m of margin for additional errors like alignment tolerances or inaccuracies of the mount model.

$$r = l \cdot \tan(\theta) \tag{2}$$

This relatively large divergence results in a reduced power density at the spacecraft. To overcome this lack of power and to close the link budget, two erbium doped fiber amplifiers (EDFA) are used to amplify the light of each beacon and generate an output power of 4 W each.

3.3 Receiver

The OGSOP-NG is equipped with several cameras, visual and infrared (IR). An external IR-camera was used for tracking the satellite during the PIXL-1 mission. This means the camera was attached on top of the telescope so that the light it received did not go through the telescope itself. The received optical power by the camera is much lower than the received power by the telescope, but the power density of O4C on ground is high enough, that the spot can easily be detected on the IR image. Image processing of the IR-camera picture is used for fine tracking. If a constant signal is received by the camera, the ground station tracks on the acquired spot image and no longer on the orbit file. This increases the accuracy of OGSOP-NG significantly.
The receiver used for O4C is attached at the so called “shark-fin setup” and does not use the coudé-path. The shark-fin is an optical bench on top of the OGSOP-NG, which can be seen in Figure 6. This minimizes possible losses caused by the coudé-path, because the light gets coupled out of the telescope through the upper Nasmyth-port and is focused directly on the receiver front end (RFE).

Figure 6. Shark-fin on upper Nasmyth-port of OGSOP-NG (green circle)

To guarantee that the all the received light reaches the RFE, the tracking target in the IR image and the focus of the telescope must be perfectly aligned to the RFE. To check and verify this before every experiment DLR can use a test laser installed in a telecommunication tower in 6.4 km distance.

The output of the RFE is attached to the Receiver electrical ground support equipment (Rx-EGSE), which is an in-house development of DLR. Inside of the RFE is an avalanche photo diode (APD) which does the optical-electrical current conversion. The electronics behind transfer the electrical current into a voltage. The signal transmit by O4C is modulated with optical on-off-keying (O3K), which means laser ON is interpreted as a binary 1 and laser OFF as binary 0. These ones and zeros are transferred from the RFE to the Rx-EGSE. The Rx-EGSE receives the signal, recovers the clock automatically and decodes the data. Afterwards the original data (in case of PIXL-1 pictures) are stored on a SD-card inside the Rx-EGSE.

4 DOWNLINK CAMPAIGN – PIXL-1

The PIXL-1 mission began on the 24th of January 2021. On this day CubeL started onboard a Falcon 9 as part of the Transporter 1 mission and was deployed into a sun-synchronous orbit with an apogee of 514 km. DLR started after launch and early orbit phase (LEOP) and commissioning with first laser experiments. The verification of the terminal followed a strategic error reduction and pointing improvement with the following steps:

1. AOCS check out
   - Verify Pointing to celestial body (Earth's moon)
2. Target pointing
   - without offset
   - with offset to increase area of interest
3. Offset compensation
   - Using satellite telemetry (TM)
   - Using O4C TM

Base for all the steps described above is a reliable reference, which is in case of CubeL the star tracker as the most accurate absolute sensor in the AOCS. The steps and the actions performed by DLR are described in the following subchapters.

4.1 AOCS check out

The first steps in the LEOP were to check out every subsystem of the satellite. The satellite manufacturer GomSpace took over the LEOP and tested all relevant subsystems, as precondition for DLR to start with laser experiments. To verify the pointing of CubeL the satellite pointed with the camera to the moon and took pictures of, which were downloaded afterwards. After the images were taken, the following image processing methods have been applied to estimate the centroid of the Moon with respect to the image frame

1. Grayscale image from RGB image
2. Otsu thresholding to filter background
3. Connected component labelling to choose the biggest object in the image after thresholding
4. Canny edge detection to detect the edge around the object
5. Hough circle transform to estimate circles based on detected edges

From step 5, the best estimated circle with largest radius is taken to find the centroid of the moon. This is to avoid smaller circles generated when the Moon is only partially illuminated (e.g. crescent moon). An example of post-processed image is shown in Figure 7.

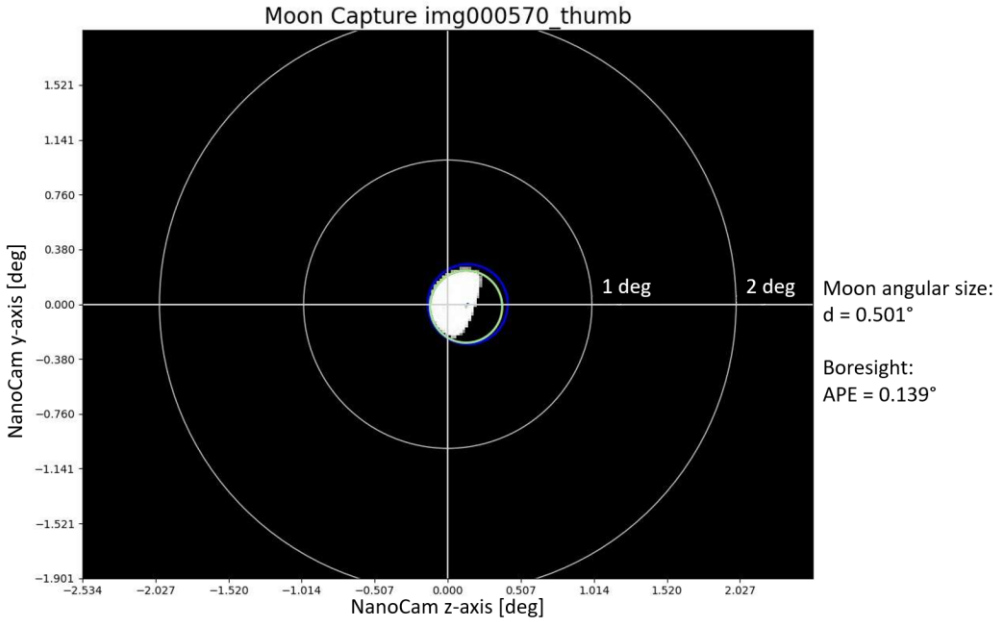

Figure 7. Post-processed moon capture and calculated boresight APE

The boresight APE is defined as the angular difference between the center of the moon and the center of the camera detector. In total 18 pictures were taken in total where nine where taken eleven hours apart from the other nine. The pictures were taken with the uncalibrated star tracker based on the computer aided design (CAD) model and the total average of the boresight APE was calculated, which can be seen in Table 1.

IMG Number	Boresight APE [deg]	IMG Number	Boresight APE [deg]
549	0.168	558	0.086
550	0.168	559	0.104
551	0.168	560	0.151
552	0.230	561	0.188
553	0.292	562	0.151
554	0.250	563	0.188
555	0.166	564	0.153
556	0.171	565	0.250
557	0.208	566	0.232
Average	0.202	Average	0.178
		Total Average	**0.190**

Table 1. Boresight APE measurement based on moon pictures

Afterwards the star tracker was calibrated to the moon and another verification measurement of seven pictures was done. The result was a further reduction of the boresight APE to a total average of 0.140°. The APE of 0.140° is lower than the FoR of O4C and fulfils the requirements of the mission. In this scenario the slew rates are lower compared to target pointing mode, so we proceeded with tests in target pointing mode to verify the behavior in the final scenario.

4.2 Target pointing

The results of the moon campaign proofed that the AOCS is theoretically able to point within the required margins and that the star tracker's coordinate system is calibrated to the spacecraft's reference frame. In the first laser experiments, the satellite pointed with O4C to the OGS based on the CAD model of the satellite, which does not consider misalignments between O4C and the reference frame. During the first tests the beacons were not included in the operation which means, the spiral of O4C swipes over the OGS which can be observed as flashes at the image of the IR-camera. The time distance between the flashes was round about 8 s (it differs if the satellites attitude changes between two spirals) which is the exact time of one duration of the FSM spiral depicted in Figure 1.

We correlated the time stamps of the flashes of the successful links with the TM of the AOCS, after it was downloaded. Unfortunately, during none of the successful links did the star tracker have a valid lock. Without a reliable sensor reference of the AOCS, the information of the star tracker, it is impossible to estimate or calculate the pointing offset or to reproduce the links, independent from the calculated boresight APE of the AOCS. During the very limited times where the star tracker had a valid lock and the boresight APE was reduced to below 1°, no flashes were observed at the OGS. This led to the conclusion that the misalignment between O4C and the reference frame is larger than 1° and has to be compensated by a pointing offset. These misalignments could be caused e. g. by settling effects during launch and could lead to deviations in the alignment of several degrees.

The idea to measure the pointing offset is to apply an angular offset to the satellites attitude, which represents a change in target by maximum 1°, that the spirals driven by the FSM overlap on ground. Adding multiple targets increase the search area to find the correct pointing offset. Figure 8 shows one example search pattern where the green circle marks the original pointing target (OGS). The circles with a radius of 1° represent the FoR of O4C and the area covered by the FSM's spiral. With changing the targets position during the link, a larger area (yellow) can be covered during one flyover. It has to be guaranteed that at least two full durations of one spiral (8 s) are performed, before the

satellite changes the attitude to the next target.

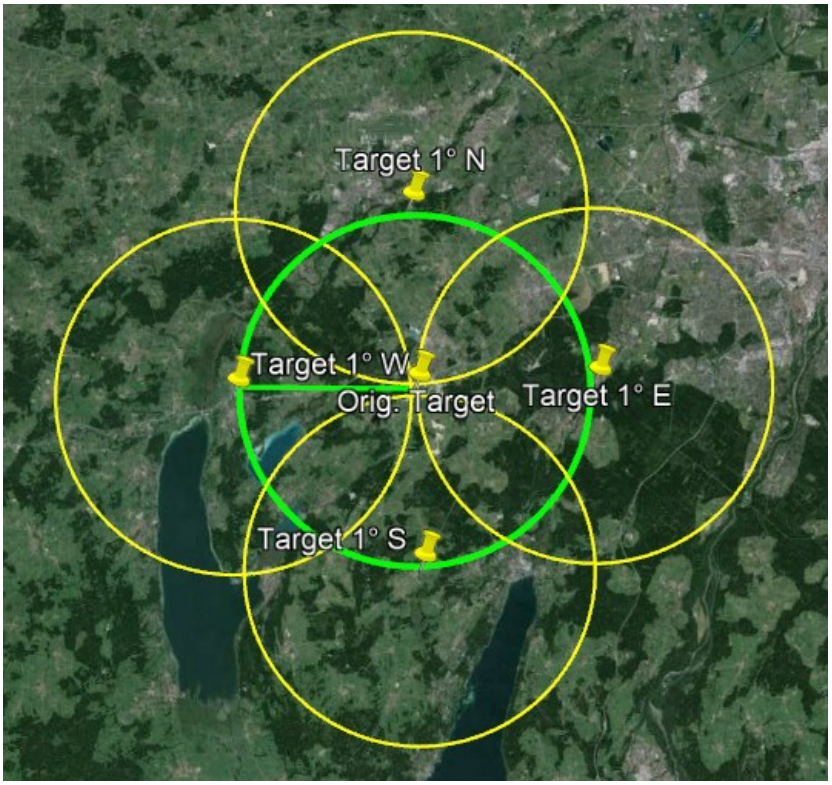

Figure 8. Search pattern with overlapping 1° radius circles

Search procedures like these were already approved in former projects like OSIRISv1 with Flying Laptop [8]. To correlate the data after the laser experiments with the AOCS TM, a reliable reference is required. It turned out that during none of the links the star tracker was available over the whole pass, independent from the maximum elevation or the orientation of the satellite. Without a reliable absolute reference, it is impossible to tell if the satellite is pointing to the assumed location or not, independent from the observations at the OGS.

These issues with this specific star tracker are already known from other missions [9]. Software solutions were discussed, but the star tracker is not able to be updated via software upload in space. Thus, the required changes to increase the availability of the star tracker had to be done via parameters during the commanding. The behavior could be improved that the star tracker was afterwards available during links with a maximum elevation of up to ~45°. This fits to the data sheet of the star tracker and was considered in the operations concept of CubeL's AOCS by relying on the gyro sensors after a star tracker drop out to keep the boresight APE below 1°. After stabilizing the star tracker, further experiments showed that the star tracker cannot operate in some specific sky regions at all. During laser communication there is only one degree of freedom, the optical axis. Considering the celestial bodies, the sun, the moon and the earth, which has to be excluded of the Field of View (FoV) of the star tracker, excluding additional sky regions would be too complicated and had to be calculated individually for every flyover. This limits the availability of the star tracker and with that the number of usable downlinks significantly.

4.3 Offset compensation

Nevertheless, we continued with laser experiments after having at least a chance of a flyover with a valid star tracker lock over parts of the link. As the star tracker was still not reliable during a whole pass, search patterns with changing targets within one flyover were not reasonable. Thus, constant

offsets were applied for a full link, changing after every experiment which increased the number of experiments. Flashes were observed in some of the downlink experiments, shortly after the star tracker lost its lock, which could be seen after the TM was downloaded. This indicates that the pointing offset was still incorrect. We could use the information of the assumed movement of the satellite after the lost lock to calculate a new pointing offset. Due to the limited bandwidth of the UHF telecommunication channel, the sample rate of the TM had to be reduced to 0.1 Hz. This led to a couple of iterations to improve the pointing offset. We could verify the target pointing as signals were always observed when the star tracker was available and the satellite reduced the boresight error below 1°.

During the PIXL-1 mission it was not possible to frequently download GPS-data from CubeL, because of a limited power budget. Thus, Two-Line-Elements (TLE) had to be used as orbit files for the OGSOP-NG. TLEs are less accurate than GPS-based orbit files. The TLEs are generated only once per day so it is possible that the TLE can be up to 24 hours old. Propagated errors can lead to an inaccuracy of the orbit file larger than the spot radius of the beacon described in chapter 3.2. This issue could be solved by an image processing algorithm inside the OGSOP-NG. The offset caused by the inaccuracy of the TLE is larger than the beacons spot, but it is smaller than the FoV of the IR-camera. During the acquisition phase O4C drives spirals with the FSM as shown in Figure 1. If one of these spiral arms swipes over the OGS, the signal can be seen as flash on the camera image. As soon as the camera detects a flash the offset between flash and target is automatically calculated and can be compensated by the OGSOP-NG. Afterwards, O4C can acquire the beacon during the next revolution of the spiral (after 8 s).

On the 13th of June 2023 DLR could for the first time establish a stable tracking connection between the OGSOP-NG and O4C. After a short bad weather period, this success could be repeated on the 25th of June. The TM collected by CubeL of this downlink is shown in Figure 9 and discussed in the following.

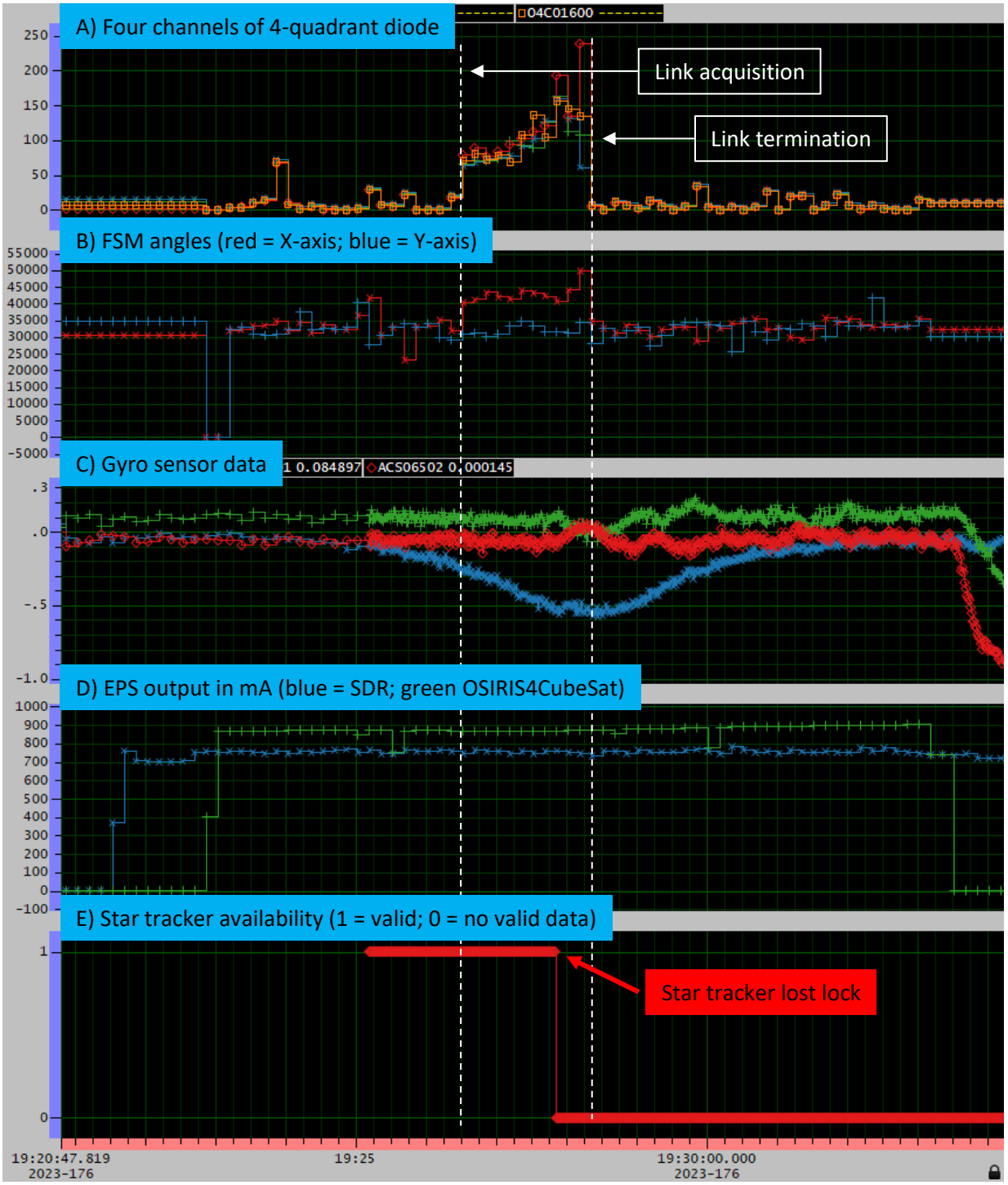

Figure 9. CubeL telemetry of first tracking

The TM is sampled with 0.1 Hz except the ADCS TM which includes the gyro sensor data and the star tracker valid parameter, they are sampled with 1 Hz. In the beginning of the flyover, CubeL has to stabilize itself to reduce the pointing error to below 1°. The first flash was observed at 19:25:59. Afterwards the pointing of the OGSOP-NG was corrected, using the procedure described above, so that the beacons hit the satellite. O4C acquired the beacon 16 seconds later and had a stable tracking for 1 minute and 48 seconds. This can be seen in plot A) which shows that the 4QD received light on all four quadrants. Unfortunately, the star tracker dropped out at 19:27.51, which can be seen in plot E). The loss of the star tracker resulted in a drift of the satellite around one axis. The FSM compensated, based on the received signal of the 4QD, this drift until it reached its mechanical limit, which can be seen in the red curve of plot B).

O4C samples the data internally with 200 Hz. Thus, we downloaded the internal TM of this link which proofed the behavior indicated by the low-sampled TM from CubeL. Figure 10 shows the FSM behavior in more detail.

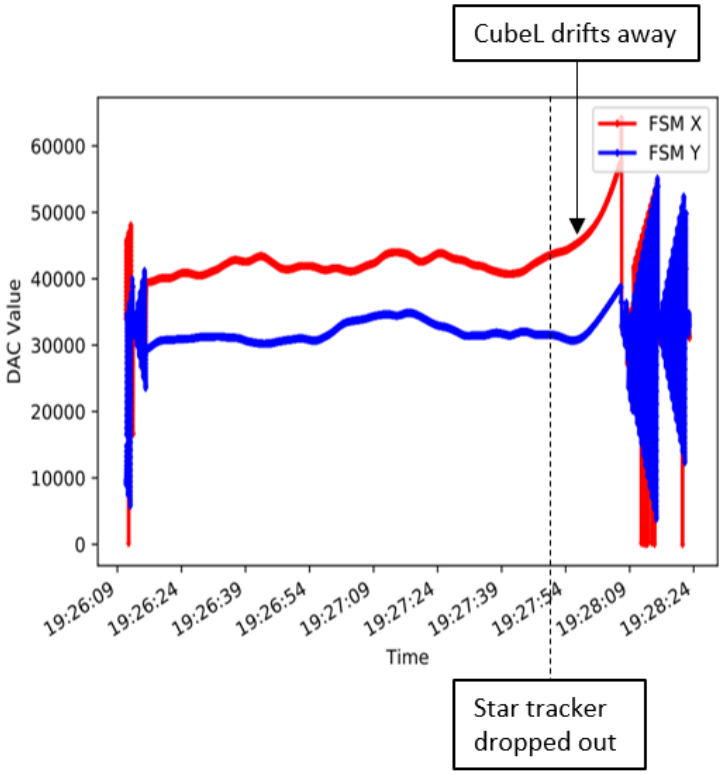

Figure 10. FSM tilt during laser experiment

After the FSM reached its mechanical limit in the X-axis, it started spiraling again, searching for the beacon. The link was terminated at maximum elevation of 42° which can be seen based on the gyro data in plot C) of Figure 9.

The offset between X- and Y-axis of the FSM during tracking, visible in Figure 10 indicates that the adapted target pointing offset still has room for improvement. We took the results of this and the following successful links to further improve the pointing. This did not have an effect on the availability of the star tracker and so did not increase the number of laser experiments being possible, but it increased the stability during the link and increased the duration of the optical connection to several minutes in some of the links.

4.4 End-to-end Transmission

Until this O4C sent only dummy data as the first step was to demonstrate the successful and stable tracking as a reliable base for data transfer. Afterwards we switched to data transfer, captured and encoded a picture of Munich. On the 15th of September we could downlink the first picture, taken by CubeL and transmitted via O4C.

Figure 11. First picture transmitted via O4C

The picture shows the metropolitan area of Munich, Germany taken from the southeast. Especially the river Isar and the Munich airport can easily be recognized. The great success does nit lie in the picture itself. It is the first time that the full transmission chain in an end-to-end scenario could be verified. The picture was taken by the NanoCam, encoded on board of CubeL, transmitted by O4C via laser to the OGSOP-NG, received by the RFE and decoded in the Rx-EGSE. Never before did all distinguished subsystems work together. This demonstration is very close to an operational scenario and proves that O4C is ready for the industry.

5 CONCLUSION

The paper gives a very broad overview of the OSIRIS4CubeSat payload onboard the CubeL satellite and the demonstrator mission PIXL-1. It covers the space segment, consisting of the satellite and the payload but also the ground segment as an essential part of the end-to-end communication, which has been demonstrated from image taking on the satellite, channel coding, transmission, reception on ground and decoding. During the experiments, the ADCS proved to be very challenging: the optical payload uses the CubeL satellite as coarse pointing assembly - with the shortcomings of the used star tracker, it is a challenge the keep the orientation towards the ground station. A huge effort has been invested into the star tracker and ADCS to make the demonstration mission a successful basis for coming missions.
The developed and demonstrated optical terminal is the basis for further missions: QUBE is expected to be launched in summer 2024 and will demonstrate quantum experiments on a CubeSat to pave the way for QUBE-II with an 85 mm telescope to implement and demonstrate a quantum key distribution from a CubeSat in 2025. Furthermore, the optical system is also part of the CubeISL demonstration mission between two CubeSats in 1.500 km maximum distance with a bidirectional 100 Mbps optical link. On this basis, the optical payload for the SeRANIS mission will incorporate a dedicated coarse pointing assembly to decouple the payload from the satellite’s ADCS system and operation of other payloads like imaging.

6 REFERENCES

[1] Martin Pimentel, Patricia und Rödiger, Benjamin, et. al. *Cube Laser Communication Terminal (CubeLCT) state of the Art,* Acta Astronautica, Elsevier. doi: 10.1016/j.actaastro.2023.06.026, ISSN 0094-5765, 2023

[2] Alberto Carrasco-Casado, Hideki Takenaka, et. al. *LEO-to-ground optical communications using SOTA (Small Optical TrAnsponder) – Payload verification results and experiments on space quantum communications,* Acta Astronautica, Elsevier, Volume 139, 2017, Pages 377-384, ISSN 0094-5765,

[3] D. Giggenbach, C. Fuchs, et. al., *Downlink communication experiments with OSIRISv1 laser terminal onboard Flying Laptop satellite,* In: Applied Optics 61, pp. 1938–1946. 2022

[4] Giggenbach, Dirk und Shrestha, Amita et. al. *SYSTEM ASPECTS OF OPTICAL LEO-TO-GROUND LINKS*, In: ICSO Proceedings. International Conference on Space Optics, 18-21 Okt. 2016, Biarritz. doi: 10.1117/12.2296054, 2016

[5] Erik Kulu, *Nanosat Database*, [online], Available: https://www.nanosats.eu/img/fig/Nanosats_years_types_2023-12-31.pdf, 2024, January 1

[6] Prell, Johannes und Duliu, Alexandru-Octavian, et. al. (2023) *Optical Ground Station Oberpfaffenhofen Next Generation: first satellite link tests with 80 cm telescope and AO system.* In: IEEE International Conference on Space Optical Systems and Applications, IEEE International Conference on Space Optical Systems and Applications, 2023

[7] Fuchs, Christian, *Transmitter Diversity with Phase-Division in Bit-Time,* Dissertation, Christian-Albrechts-Universität zu Kiel. doi: 10.2370/9783844082135, 2021

[8] Fuchs, Christian und Schmidt, Christopher, et. al. *Update on DLR's OSIRIS program and first results of OSIRISv1 on Flying Laptop,* In: Proceedings of SPIE - The International Society for Optical Engineering, page 27, San Francisco, doi: 10.1117/12.2514349, ISBN 978-151062462-7, ISSN 0277-786X, 2019

[9] Nowak, Mathias, et al. *Short life and abrupt death of PicSat, a small 3U CubeSat dreaming of exoplanet detection,* Space Telescopes and Instrumentation 2018: Optical, Infrared, and Millimeter Wave. Vol. 10698. SPIE, 2018.